Role of Naphthenic Acids in Emulsion Tightness for a Low-Total-Acid-Number (TAN)/High-Asphaltenes Oil

ARTICLE *in* ENERGY & FUELS · MARCH 2009

Impact Factor: 2.79 · DOI: 10.1021/Ef800615e

7 AUTHORS, INCLUDING:

Vincent Pauchard
SINTEF
18 PUBLICATIONS **228** CITATIONS
SEE PROFILE

Sunil Kokal
Saudi Arabian Oil Company
54 PUBLICATIONS **611** CITATIONS
SEE PROFILE

Hendrik Muller
Saudi Arabian Oil Company
29 PUBLICATIONS **150** CITATIONS
SEE PROFILE

Adnan Al-Hajji
Saudi Arabian Oil Company
63 PUBLICATIONS **256** CITATIONS
SEE PROFILE

Role of Naphthenic Acids in Emulsion Tightness for a Low-Total-Acid-Number (TAN)/High-Asphaltenes Oil†

Vincent Pauchard,*,‡ Johan Sjöblom,§ Sunil Kokal,‡ Patrick Bouriat,|| Christophe Dicharry,|| Hendrik Müller,‡ and Adnan al-Hajji‡

Research and Development Center, Saudi Aramco, Dhahran 31311, Saudi Arabia, Ugelstad Laboratory, Norwegian University of Technology, Trondheim NO-7491, Norway, and Laboratoire des Fluides Complexes, UMR CNRS 5150, Université de Pau, BP 1155, 64013 Pau Cedex, France

Received July 30, 2008. Revised Manuscript Received October 20, 2008

The emulsion stabilizing properties of a low-total-acid-number (TAN) crude oil, which had initially been attributed to asphaltenes and calcite precipitation, were re-analyzed with regard to the role of organic acids. Despite high asphaltenes content, this crude oil exhibits features classically observed with acidic oils, such as the increase in emulsion stability upon pressure decrease/pH increase or the poor efficiency of demulsifiers. The potential for a significant role of organic acids was confirmed by the high interfacial activity of indigenous acids, as extracted from the crude oil by means of an ion-exchange resin. This was further addressed analyzing the molecular chemistry of the interfacial layer and its rheology. The interfacial material was found to be composed of a mixture of asphaltenes and organic acids. These acids exhibit a wide range of structures (mono- versus dicarboxylic, fatty versus naphthenic and benzoic) and molecular weights (from 200 to 700 g/mol), contrary to the medium molecular weight fatty monocarboxylic acids that are generally believed to cause "soap emulsions". The interfacial rheology is indicative of a 2D gel, with an assumed glass transition temperature of approximately 40 °C. In conclusion, this study shows that a co-precipitation of asphaltenes and organic acids can promote the build up of a very cohesive interface. The disruption of this interface not only requires the drainage of individual molecules but also a collective yield of the gel. This paper is part one of two: it confronts physical and chemical data, the latter being further detailed in an associated paper.

Introduction

The considered crude oil is of Arab Medium quality [American Petroleum Institute (API)° 27] and is produced from a large offshore field. It had already been studied with regard to emulsion problems from the wellbore to the final onshore processing plant.

A first study[1] of the fouling of offshore facilities by a sludge emulsion had resulted in the recommendation of a small injection (1 ppm) of demulsifier. The emulsion tightness was at the time attributed to the presence of fine solids.

A second study[2] focused on the emulsion behavior in the reservoir and the wellbore. Wellbore samples were collected using a pressure-compensated piston chamber and transferred into a transparent pressure−volume−temperature (PVT) cell equipped with a built-in stirrer. The effect of pressure decay on emulsion stability was then visually monitored. A first increase in emulsion stability observed at the bubble point pressure was attributed to asphaltenes precipitation. A second increase in emulsion stability upon further pressure decrease below the bubble point was attributed to calcite precipitation upon pH increase. These conclusions were drawn based on the scanning electron microscopy (SEM) analysis of the solids extracted from emulsions, revealing some crystals of calcite and sodium chloride in a sulfur-rich hydrocarbon matrix.

Table 1. Main Oil and Emulsion Characteristics[a]

API°	27	water cut in sample (vol %)	7
$C20^-/C20^+$ (wt %)	40/60	separated water in sample (vol %)	0
asphaltenes (wt %)	7.3	droplets size $d_{v,50}$ (μm)	4
TAN (mg of KOH/g)	0.24	total dissolved salts (g/L)	210
viscosity at 60 °C (mPa s)	6.0	solid residue in dichloromethane (%)	13

[a] Data published under courtesy of refs 3 and 4.

A third study[3,4] addressed the systematic characterization of Saudi Aramco crude oils and their associated emulsions with respect to the water separation processes. The conclusions regarding the oil in the focus of the present paper was again that the emulsion tightness was probably due to asphaltenes and fine particles. Relevant results are summarized in Table 1.

Recently, the presence of fine particles was further investigated by treating a sludge emulsion with large volumes of tetrahydrofuran, which dissolved the sample with the exception

† Presented at the 9th International Conference on Petroleum Phase Behavior and Fouling.

* To whom correspondence should be addressed. Telephone: (966) 3-872-5117. Fax: (966) 3-876-8870. E-mail: vincent.pauchard@aramco.com.

‡ Saudi Aramco.

§ Norwegian University of Technology.

|| Université de Pau.

(1) Kokal, S.; Al-Yousif, A.; Meeranpillai, N. S.; Al-Awaisi, M. Presented at the Society of Petroleum Engineers (SPE) Annual Technical Conference and Exhibition (ATCE), New Orleans, LA, Oct 2001; SPE paper 71467.

(2) Kokal, S.; Al Dhoki, M. Presented at the 15th Society of Petroleum Engineers (SPE) Middle East Oil and Gas Show and Conference, Bahrain, March 2007; SPE paper 105534.

(3) Al Ghamdi, A. M.; Noïk, C.; Dalmazzone, C.; Kokal, S. Presented at the 2007 Society of Petroleum Engineers (SPE) International Symposium on Oilfield Chemistry, Houston, TX, March 2007; SPE paper 106128.

(4) Al Ghamdi, A. M.; Noïk, C.; Dalmazzone, C.; Kokal, S. Presented at the Society of Petroleum Engineers (SPE) Annual Technical Conference and Exhibition (ATCE), Anaheim, CA, Nov 2007; SPE paper 109888.

10.1021/ef800615e CCC: $40.75
Published on Web 12/03/2008

Table 2. Brine Analysis and Main Parameters of the Scale Simulations

crude oil flow rate (MMBD)	1.4
water flow rate (MBD)	90
gas flow rate (BCFD)	0.4
Na^+ in water (g/L)	50
Ca^{2+} in water (g/L)	10
Cl^- in water (g/L)	100
HCO_3 in water (mg/L)	60
CO_2 in gas (mol %)	1
temperature (°C)	60

Table 3. Main Results of the Scale Simulations

pressure (MPa)	20	6	3	0.1
pH	4.86	5	5.3	6.8
precipitated calcite and gypsum (kg/day)	0	0	0	1

Figure 1. Water separation in emulsions made of brines with initial pH values of 5, 7, and 8 (left to right). After a few weeks, the pH 5 sample is divided into three equal parts: free oil, rag layer, and free water (top to bottom). At pH 7, the rag layer represents one-half of the total volume. At pH 8, the rag layer represents two-thirds of the total volume and there is almost no free water.

of a few particles of iron oxide. This experiment disqualified the calcite particles as a possible cause for emulsion tightness. It is probable that the crystals previously observed had precipitated during the drying of the solid residue of the emulsion because of an incomplete water separation. The same procedure was repeated with lower volumes of tetrahydrofuran, and a rag layer appeared. The elemental composition of this layer was found to differ significantly from the one of the crude oil and its asphaltenes. The rag layer contains more oxygen (3−17% atomic compared to 0.3 and 4% atomic in oil and asphaltenes, respectively) and less sulfur (1−4% atomic compared to 2.6 and 5.5% atomic in oil and asphaltenes, respectively). The impossibility to match the rag layer composition with a mixture law of oil and asphaltenes compositions suggests a selective adsorption of some particular asphaltenes and/or other oxygenated components.

The influence of calcite precipitation was finally disqualified by water chemistry analysis and scale simulations using Multiscale. Given the low carbonate content (Table 2), the pH value of the brine only reaches 6.5 at atmospheric pressure (which was confirmed by measurements on produced water) and the amount of precipitated calcite is below 0.1 ppm with respect to the total fluids (Table 3).

Finally, the emulsion stability was investigated at various pH values for artificial brines without carbonates. It was found that the emulsion tightness increases with a pH increase between 5 and 8 (Figure 1). Such an evolution is an indication of the influence of carboxylic acids rather than of the influence of asphaltenes. The stability of emulsions made of asphaltenic oils or bitumen is often reported to be lower at neutral pH than at acidic pH (probably because of the basic nature of many asphaltenes).[5−7] Contrarily, carboxylic acids are reported to cause problems at neutral pH because their dissociation constant (pK_a) is around 5. The type of problem encountered depends upon the acid type:[8] (i) very tight emulsions ("soap emulsions") stabilized by the salts of fatty acids with molecular weights ranging from 200 to 400 g/mol,[9] (ii) high content of soluble hydrocarbons in produced water because of the water-soluble salts of aliphatic acids of low molecular weight,[10] and (iii) fouling deposits formed by the polymeric salts of tetracarboxylic acids.[11]

It is now admitted that, in the worst "soap emulsions", encountered with light crude oils, fatty acids develop interactions with paraffins to form a very resistant interface.[12,13] Contrarily, the interactions between asphaltenes and acids in medium and heavy crude oils have not been extensively investigated. It was sometimes assumed that organic acids compete with asphaltenes for interfacial adsorption, leading to a decrease in emulsion tightness at neutral pH.[14] Contrarily, a direct study of the interfacial material extracted from water in bitumen emulsions showed a significant contribution of carboxylate salts mixed with asphaltenes.[15,16] Very recently, a new consensus arose at the 9th Petrophase Conference pin-pointing that organic acids and asphaltenes may co-precipitate or co-adsorb at the water−oil interface, increasing the interface resistance.[17−22]

The results presented in this paper are very consistent with the above-mentioned consensus. They exemplify the influence of organic acids on the behavior of a low-total-acid-number

(5) Poteau, S.; Argillier, J.-F.; Langevin, D.; Pincet, F.; Perez, E. *Energy Fuels* **2005**, *19*, 1337–1341.
(6) McLean, J. D.; Kilpatrick, P. K. *J. Colloid Interface Sci.* **1997**, *1892*, 242–253.
(7) Chaverot, P.; Cagna, A.; Rondelez, F. Dilational rheology of bitumen−water interfaces: Influence of asphaltene surfactants at acidic and neutral pH. Presented at the 9th Petrophase Conference, Vancouver, British Columbia, Canada, June 2008.
(8) Hurtevent, C.; Ubbels, S. J. Presented at the 2006 Society of Petroleum Engineers (SPE) International Oilfield Scale Symposium, Aberdeen, Scotland, June 2006; SPE paper 100430.
(9) Ubbels, S. J.; Turner, M. Diagnosing and preventing naphthenate stabilized emulsions during crude oil processing. Presented at the 6th Petrophase Conference, Amsterdam, The Netherlands, June 2005.
(10) Hurtevent, C.; Rousseau, G.; Goldszal, A. Presented at the 5th International Symposium on Oilfield Scale, Aberdeen, Scotland, Jan 2003; SPE paper 74661.
(11) Baugh, T. D.; Grande, K.; Mediaas, H.; Vinstad, J. E.; Wolf, O. Presented at the Society of Petroleum Engineers (SPE) 7th International Symposium on Oilfield Scale, Aberdeen, Scotland, May 2005; SPE paper 93011.
(12) Brocart, B.; Hurtevent, C. Focus on fatty acids and waxes in sludge emulsion formation. Presented at the Society of Petroleum Engineers (SPE) Workshop Managing Naphthenates and Soap Emulsions, Pau, France, March 2008.
(13) Gallup, D. L.; Curiale, J. A.; Smith, P. C. *Energy Fuels* **2007**, *21* (3), 1741–1759.
(14) Arla, D.; Sinquin, A.; Palermo, T.; Hurtevent, C.; Graciaa, A.; Dicharry, C. *Energy Fuels* **2007**, *21* (2), 1337–1342.
(15) Wu, X. A. *Energy Fuels* **2003**, *17* (1), 179–190.
(16) Stanford, L. A.; Rodgers, R. P.; Marshall, A. G.; Czarnecki, J.; Wu, X. A. *Energy Fuels* **2007**, *21* (2), 963–972.
(17) Moran, K.; Kiran, S.; Acosta, E. The formation of rag layers and the role of interfacial partition of naphthenates and asphaltenes. Presented at the 9th Petrophase Conference, Vancouver, British Columbia, Canada, June 2008.
(18) Baydak, E. N.; Yarranton, H. W.; Ortiz, D.; Moran, K. Effect of demulsifiers on interfacial films and stability of water-in-oil emulsions stabilized by asphaltenes. Presented at the 9th Petrophase Conference, Vancouver, British Columbia, Canada, June 2008.
(19) Czarnecki, J. On the stabilization of water in crude oil emulsions. Presented at the 9th Petrophase Conference, Vancouver, British Columbia, Canada, June 2008.
(20) Ehrmann, B. M.; Juyal, P.; Rodgers, R. P.; Marshall, A. G. An investigation of emulsion interfacial material by ultrahigh resolution FT-ICR mass spectrometry. Presented at the 9th Petrophase Conference, Vancouver, British Columbia, Canada, June 2008.

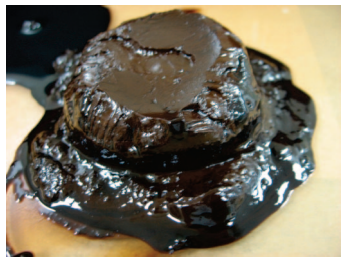

Figure 2. Sludge emulsion collected at the bottom of a sampling bottle after a few weeks of long settling. The sludge is paste-like and does not flow because of a very high water cut (up to 85 vol %).

(TAN)/high-asphaltenes crude oil with respect to interfacial chemistry and interface behavior. More details on the analytical chemistry investigation can be found in ref 23.

Experimental Materials

Fluid Sampling. Samples of mixed water and crude oil were collected at the inlet of the onshore processing plant. The sampling point was located on the trunk line upstream of the demulsifier injection point (but of course downstream of the offshore injection of 1 ppm demulsifier). The fluids were directly poured from a 5 bar production line into an open jerry can. The water cut in the samples ranged from 1 to 10% volume. No phase separation was observed, with water rather being dispersed under the form of micrometer-size droplets. It is not known for certain if the small water droplet size is due to shearing during sampling or flow conditions in the production line. Given the intrinsic mechanical resistance of the interfacial layer (as presented in the Results), it is believed that shearing during sampling is not likely to instantaneously produce small droplets.

Gravity Separation. Mixed fluid samples were left at rest for a few weeks. This resulted in a clear separation into two phases: supernatant oil and sludge emulsion. The sludge emulsion was either a very viscous fluid containing ca. 25% water or a paste-like solid containing up to 85 vol % water (Figure 2), depending upon the total water cut of the sample.

The chemistry of the supernatant oil was characterized by Fourier transform ion cyclotron resonance mass spectrometry (FT-ICR MS). The oil was also used for experiments (interfacial rheology and emulsion stability) and extractions (acids and asphaltenes).

The most concentrated sludge emulsion was characterized by Fourier transform infrared spectroscopy (FTIR) and used for extractions. It is hereafter called "whole interfacial material", although it contained up to 85% of water and some supernatant oil. It was preferred not to further eliminate the supernatant oil because any treatment might have altered the chemical composition of the intrinsic interfacial material. The discussion of the results accounts for the presence of entrapped oil.

Extraction of Indigenous Acids by Ion-Exchange Resin (IER). The organic acids contained in the supernatant oil were extracted by the acid IER method developed by Mediaas et al.[24] The resin was a QAE Sephadex A-25 activated by a Na_2CO_3/$NaHCO_3$ buffer solution, rinsed with deionized water, and saturated with methanol. The activated resin was mixed with 100 mL of crude oil and 200 mL of toluene for 16 h to trap the organic acids. The charged resin was then washed thoroughly with toluene and methanol until the filtrate was colorless to remove any non-acidic component. The cleaned resin was further stirred with a mixture of toluene, methanol, and formic acid to release the organic acids. After multiple washings, the extracted acids were separated from solvents and formic acid by evaporation (rotavapor 60 °C, 120 rpm). The yield was 0.05 wt % with respect to oil. The extracted indigenous acids were used for interfacial activity characterization.

Extraction of Indigenous Acids by Ammonia Bubbling. The organic acids contained in the supernatant oil were also extracted by a concentration method developed by Mapolelo et al.[25] The oil was bubbled with gaseous ammonia to convert any acidic species into ammonium salts. The oil was then refrigerated to cause ammonium salts to precipitate as a salt sludge. These solids were collected by filtration and dissolved in toluene or methanol. The extracted indigenous acids were used for FT-ICR MS characterization.

Extraction of Interfacial Material Subfractions. The whole interfacial material was washed by elution with solvents, such as toluene. This resulted into two samples: a solution of the species poorly bonded to the interface and a cleaned (almost white) emulsion containing only the species strongly bonded to the interface.

The material remaining in the cleaned emulsion is hereafter called "strongly bonded interfacial material". It was further dried for FTIR characterization or treated with a strong acid for FT-ICR MS characterization. In the later case, following the preparation method developed by Mediaas et al.[24] for naphthenates deposits, a sample of cleaned emulsion was put in between large volumes of hydrochloric acid (1 mol/L) and toluene for 24 h. The released species were collected from the toluene phase.

The eluted species, hereafter called "poorly bonded interfacial material", were characterized by means of FT-ICR MS, FTIR, and asphaltenes extraction. It is noteworthy that the "poorly bonded interfacial material" contains some supernatant oil just as the whole interfacial material.

Asphaltenes Extraction. Asphaltenes were extracted from both the supernatant oil and the "poorly bonded interfacial material". A sample of 0.5 g was mixed with 20 mL of *n*-pentane. After refrigeration for 72 h, the precipitated asphaltenes were filtered on a number 40 Whatmann filter paper and washed thoroughly with *n*-pentane. After drying, asphaltenes were weighed and dissolved in toluene. The asphaltenes extracted from the supernatant oil were further characterized by means of FT-ICR MS and FTIR.

Experimental Methods

FTIR. FTIR aims at characterizing the chemical functional groups present on molecules. Each chemical function will absorb IR energy at specific ranges of wavenumber, therefore allowing for its identification. This identification may be difficult because the adsorption peaks of a function may overlap with others or may be shifted because of the influence of other parts of the molecule. This is particularly true for crude oils. FTIR spectroscopy has, however, been widely used for characterizing acids,[26,27] asphaltenes,[28] and interfacial material.[15,29]

Spectra were acquired in transmission mode on a Nicolet Magna 860 spectrophotometer with a Spectratech 0002-391 diffuse reflec-

(23) Muller, H.; Pauchard, V.; al-Hajji, A.; Rodgers, R. P. The role of naphthenic acids in emulsion tightness for a low TAN/high asphaltenes oil: Characterization of the interfacial chemistry. *Energy Fuel*, manuscript submitted.

(21) Alvarez, G.; Argillier, J. F.; Langevin, D. Asphaltenes: Interfacial aggregates characterization and film structure. Presented at the 9th Petrophase Conference, Vancouver, British Columbia, Canada, June 2008.

(22) Carbonezi, C. A.; de Almeida, L. C.; Araujo, B. C.; González, G. Solution behavior of naphthenic acids and its effect on the asphaltenes precipitation onset. Presented at the 9th Petrophase Conference, Vancouver, British Columbia, Canada, June 2008.

(24) Mediaas, H.; Grande, K. V.; Hustad, B. M.; Rasch, A.; Rueslatten, H. G.; Vindstad, J. E. Presented at the 5th International Symposium on Oilfield Scale, Aberdeen, Scotland, Jan 2003; SPE paper 80404.

(25) Mapolelo, M. M.; Rodgers, R. P.; Marshall, A. G. Electrospray ionization FT-ICR mass spectrometry of "ARN" naphthenic acids in crudes: Preconcentration and quantification. Presented at the 9th Petrophase Conference, Vancouver, British Columbia, Canada, June 2008.

(26) Borgund, A.; Erstad, K.; Barth, T. *Energy Fuels* **2007**, *21* (5), 2816–2826.

(27) Brandal, Ø.; Hanneseth, A. M.; Hemmingsen, P.; Sjoblom, J.; Kim, S.; Rodgers, R. P.; Marshall, A. G. *J. Dispersion Sci. Technol.* **2006**, *27*, 295–305.

(28) Wilt, B. K.; Welch, W. T.; Rankin, J. G. *Energy Fuels* **1998**, *12* (5), 1008–1012.

(29) Petrov, A. A.; Shtof, I. K. *Chem. Technol. Fuels Oils* **1974**, *108*, 654–657.

tance infrared transmission (DRIFT) accessory. The wavenumber range was 500−4500 cm^{-1}, with a resolution of 8 cm^{-1}. Samples were pressed with highly pure KBr to form a pellet, loaded into the sample holder, and then analyzed against a pure KBr background. Samples initially containing water (sludge emulsion or cleaned emulsions) were dried overnight under a heating lamp prior to measurements.

FT-ICR MS. Mass spectra (molecular weight versus relative abundance) were acquired on a FT-ICR mass spectrometer equipped with a 9.4 T superconducting magnet.[30] This technique is based on the dependency of the rotation frequency of ionized molecules immersed in a cyclotron magnetic field on their mass and ionization number. With strong fields, the mass resolution is high enough for assigning elemental compositions ($C_xH_yN_zO_vS_w$) to most mass signals in complex mixtures. In the present case, tests were run with electrospray negative-ion mode [electrospray ionization (ESI) region], which proved to be efficient for the characterization of naphthenic acids in crude oils,[31] deposits,[11] and emulsions.[16,32] Details on the experimental procedures can be found in ref 23.

It must be noted that the relative abundance of a mass signal is not a quantitative indication of the concentration of the molecule in the sample, because of unknown response factors and interference with other molecules (so-called "matrix effect"). The comparison of the relative abundances of a given chemical class ($O_xS_yN_z$) or individual mass signal ($C_xH_yN_zO_vS_w$) within different samples can, however, provide a qualitative description of its specific presence or absence in the interfacial layer, asphaltenes, oil, etc.

Interfacial Activity of IER Extracted Acids. The notion of interfacial activity is not well-defined because it gathers different phenomenological considerations and different mechanisms. First, the apprehension of the interfacial activity of a surfactant will be intrinsically different depending upon the desired or undesired effects (emulsification versus demulsification, for example). Second, stabilization of the water/oil interface by colloids, randomly adsorbed molecules, or self-organizing molecules (or even mixed modes) will yield responses varying with the characterization techniques but not systematically correlated to the overall emulsion stability.

In the present study, the interfacial activity was rather meant as a way to compare the IER extracted indigenous acids with a commercial blend of acids from Acros Organics (Belgium) and with previously characterized model acids (naphthenic and aromatic monocarboxylic acids and tetra-carboxylic acids). We, therefore, used a previously published methodology combining dynamic interfacial tension measurements and particle formation monitoring.[33]

Dynamic interfacial tension was measured with the rising droplet method (CAM 200 KSV apparatus), which is widely used for characterizing surfactants. An oil droplet is forced into a water bath by a syringe applying a constant pressure difference between the inside and outside of the droplet. A camera meanwhile records the drop shape and dimensions. The Young−Laplace equation is then used to calculate the interfacial tension[34,35]

$$\Delta P = \gamma(1/R_1 + 1/R_2)$$

where γ is the interfacial tension, ΔP is the pressure difference, and R_1 and R_2 are the main radii of curvature of the droplet.

In the present case, the droplet constituted a toluene solution of acids, either indigenous or commercial. The indigenous acids were diluted in a concentration ranging from 0.05 to 0.14 wt %. The commercial blend was diluted in a concentration of 0.14 wt %. The water phase was a borate buffer at pH 9, with and without the addition of calcium salt to investigate the activity of carboxylic acids and carboxylate salts, respectively. In the later case, a calcium salt was added 500 s after the oil droplet had been formed.

Naphthenate particles were formed at the interface between bulk water (borate buffer solutions of pH 9.0 + 6 mM/L $CaCl_2$) and bulk toluene solutions of acids (either 0.05 wt % indigenous acids or 0.07 wt % Acros acids). Changes in optical density (OD = log{incident intensity/transmitted intensity}) of the toluene solution were monitored by a multi-purpose analyzer (Bruker Optics) equipped for transflectance measurements within the near-infrared range (9500 cm^{-1}). For dielectric particles in the Rayleigh limit, the optical density can be related to the particle formation by the following equation:[37,38]

$$\mathrm{OD} = 0.434N(\sigma_{sc} + \sigma_{abs})$$

where N is the number of particles, σ_{sc} is the scattering cross-section scaling with the sixth power of the particles radius, and σ_{abs} the absorption cross-section scaling with the third power of the particles radius.

Interfacial Rheology between Crude Oil and Artificial Brines. Interfacial rheology has become the subject of increasing interest in the emulsion science community during the past decade. In systems containing surfactants, the interface is not only a geometrical location between phases but also a finite dimension layer with an intrinsic resistance to droplet coalescence (in addition to the supernatant film drainage between two approaching droplets). As a result, it is tempting to correlate the viscoelastic response of this layer with the emulsion stability. Unfortunately, the correlations obtained with the oscillating pending droplet method are not fully satisfactory[36,39,40] and suffer from severe critics.[41] The main problems arise from the discrepancy between the experimental and real field situations (expansion of surface area versus shearing at constant interfacial area, dynamic solicitation versus quasi-static droplet coalescence, oil droplet in water versus water droplet in oil, necessity to dilute heavy oils that are the most prone to form stable emulsions, etc.). In addition, a soft material composed of a combination of functionalized or large molecules (such as naphthenic acids and asphaltenes) may exhibit complex behaviors that would not be accounted for by viscoelastic properties: thixotropy, yield strength, etc.

In the present case, the measurement of interfacial rheology parameters was primarily chosen as a tool for investigating the physical state of the interfacial layer (packing, degree of interaction between adsorbed molecules, and relative importance of elastic and viscous interactions) rather than for directly predicting the emulsion stability.

A Tracker apparatus (IT concept) was used to apply small oscillatory perturbations (less than 10% sinusoidal variation of area causing a sinusoidal interfacial tension response). In such a linear regime, Gibbs equation relates the complex interfacial dilatational elasticity E^* to the complex area variation A^* imposed by the syringe and the complex interfacial tension γ^*: $E^* = d\gamma^*/d \ln A^*$. Results are presented in terms of the interfacial dilatational modulus $E = \sqrt{(\varepsilon'^2 + \varepsilon''^2)}$ and loss angle $\phi = \tan^{-1} \varepsilon''/\varepsilon'$, with ε' and ε'' being the real and imaginary parts of E^* ($E^* = \varepsilon' + j\varepsilon''$, with $j = \sqrt{-1}$).

(30) Purcell, J. M.; Hendrickson, C. L.; Rodgers, R. P.; Marshall, A. G. *Anal. Chem.* **2006**, *78*, 5906–5912.
(31) Qian, K.; Robbins, W. K.; Hughey, C. A.; Cooper, H. J.; Rodgers, R. P.; Marshall, A. G. *Energy Fuels* **2001**, *15* (6), 1505–1511.
(32) Stanford, L. A.; Rodgers, R. P.; Marshall, A. G.; Czarnecki, J.; Wu, X. A. *Energy Fuels* **2007**, *21* (2), 963–972.
(33) Hanneseth, A. M.; Brandal, O.; Sjoblom, J. *J. Dispersion Sci. Technol.* **2006**, *27* (2), 185–192.
(34) Rotenberg, Y.; Boruvka, L.; Neumann, A. W. *J. Colloid Interface Sci.* **1983**, *931*, 169–183.
(35) Boyce, J. F.; Schurch, S.; Rotenberg, Y.; Neumann, A. W. *Colloids Surf.* **1984**, *94*, 307–317.
(37) Mullins, O. C. *Anal. Chem.* **1990**, *62*, 508–514.
(38) Kerker, M. In *The Scattering of Light and Other Electromagnetic Radiation*; Loebl, E. M., Ed.; Academic Press: New York, 1969.
(36) Hannisdal, A.; Orr, R.; Sjöblom, J. *J. Dispersion Sci. Technol.* **2007**, *28* (1), 81–93.
(39) Hannisdal, A.; Orr, R.; Sjöblom, J. *J. Dispersion Sci. Technol.* **2007**, *28* (3), 361–369.
(40) Dicharry, C.; Arla, D.; Sinquin, A.; Graciaa, A.; Bouriat, P. *J. Colloids Interface Sci.* **2006**, *297*, 785–791.
(41) Ivanova, I. B.; Danova, K. D.; Ananthapadmanabhanb, K. P.; Lips, A. *Adv. Colloid Interface Sci.* **2005**, *114−115*, 61–92.

Table 4. Test Conditions for Interfacial Rheology Measurements

test label	NaCl (g/L)	$CaCl_2 \cdot 2H_2O$ (g/L)	pH
A	0	0	5
B	0	0	7
C	0	0	8
D	33	0	7
E	185	0	7
F	0	185	7
G	145	40	5
H	145	40	7
I	145	40	8

Table 5. Experimental Conditions for Emulsion Stability Tests[a]

test label	NaCl (g/L)	$CaCl_2 \cdot 2H_2O$ (g/L)	pH
D	33	0	7
E	185	0	7
F	0	185	7
G	145	40	5
H	145	40	7
I	145	40	8

[a] Labels correspond to similar conditions in Table 4.

Experiments were at constant temperature ($T = 40$ °C) with different brines (variable pH, salinity, and cation type; see Table 4). For each test condition, rheological parameters were measured over a frequency range (0.005−0.1667 Hz). Brines were prepared by adding HCl, NaOH, $CaCl_2 \cdot 2H_2O$, and NaCl to deionized water. Crude oil was carefully homogenized prior to each experiment and could be used without dilution because of its moderate viscosity.

The first trials were performed 30 min after the formation of the oil droplet but gave erratic results. This probably resulted from the time-consuming build up and organization of the interface. The changes in the measured parameters within the duration of a frequency screening might have been too important in the case of a 30 min old interface. Actually, significant changes in interfacial tension and elastic modulus were still observed after 9 h of aging. Aging the droplet in the water bath for 16 h prior to any experiment was found to be a good compromise between measurement quality and practical considerations (e.g., solutions had to be found to avoid water evaporation). Such a long aging time is, fortunately, not too disproportional compared to the time the produced fluids actually flow from the wellhead to the separation facilities.

Emulsion Stability. Emulsion stability tests were performed using a Turbiscan Laboratory Thermo (Formulaction). It is an automated vertical-scan analyzer commonly used for monitoring settling and separation kinetics of emulsions in test tubes. A near-infrared light source combined with a double-detection system of light transmission and backscattering is used. The transmission signal allows for the detection and quantification of an increasing free water layer at the bottom of the tube. The backscattering signal allows for the detection of the dispersed water. In the case of transparent fluids, the backscattering signal can be converted into a droplet concentration profile across the height of the test tube.

Artificial emulsions made from supernatant oil (50 vol %) and artificial brines (50 vol %) were created by hand-shaking of the test tubes before introduction into the Turbiscan for up to 12 h of separation monitoring (free water detection only). The choice of hand-shaking rather than mechanical stirring was dictated by the emulsion tightness. Even with gentle mechanical stirring, artificial emulsions were so tight that no water separation was observed for days. The drawback of this choice is a certain lack of reproducibility of the results. Experiments were conducted at 60 °C for various salinities, various cation types, and various pH. Brines were prepared from reverse osmosis water by the addition of NaCl, $CaCl_2 \cdot 2H_2O$, and HCl or NaOH (Table 5).

Results

Asphaltenes and TAN. The poorly bonded interfacial material was characterized in terms of TAN and asphaltenes content. The results along with the ones obtained on the supernatant oil are reported in Table 6. It appears that the poorly bonded interfacial material is 4 times more concentrated in asphaltenes and 2 times more acidic than the supernatant oil (nevertheless, this TAN value does not capture the organic acids present under the form of carboxylate salts).

Table 6. Asphaltenes Content and TAN Value of Poorly Bonded Interfacial Material and Supernatant Oil

	asphaltenes (wt %)	TAN (mg of KOH/g)
supernatant oil	6	0.24
poorly bonded interfacial material	24	0.51

Because of the presence of supernatant oil in the sludge sample used to prepare the poorly bonded interfacial material, it is necessary to correct these results to evaluate the actual composition of the "intrinsic" poorly bonded interfacial material. The measured asphaltenes content $[\text{Asph}]_{\text{total}}$ is a mixture law of the asphaltenes contents in the oil $[\text{Asph}]_{\text{oil}}$ and the "intrinsic" poorly bonded interfacial material $[\text{Asph}]_{\text{int}}$

$$[\text{Asph}]_{\text{total}} = F_{\text{oil}}[\text{Asph}]_{\text{oil}} + (1 - F_{\text{oil}})[\text{Asph}]_{\text{int}}$$

where F_{oil} and $(1 - F_{\text{oil}})$ are the mass fractions of supernatant oil and "intrinsic" poorly bonded interfacial material in the sludge, respectively. Assuming that the oil and "intrinsic" poorly bonded interfacial material have the same density and that the "intrinsic" poorly bonded interfacial material constitutes the vast majority of the whole interfacial material (which is confirmed by the FTIR spectra), the fraction of oil F_{oil} in the sample can be evaluated as follows:

$$F_{\text{oil}} = \frac{V_{\text{oil}}}{V_{\text{oil}} + V_{\text{int}}} = \frac{V_{\text{sludge}} - (V_{\text{water}} + V_{\text{int}})}{V_{\text{sludge}} - V_{\text{water}}}$$

where V_{water}, V_{oil}, and V_{int} are the volume fractions of water, oil, and "intrinsic" poorly bonded interfacial material in the sludge emulsion. V_{water} was determined experimentally (80%), and V_{Int} can be calculated from the interface thickness δr and the mean droplet radius r (optically estimated at 4 μm)

$$V_{\text{int}} = \frac{(r + \partial r)^3 - r^3}{r^3} V_{\text{water}}$$

Assuming a reasonable upper limit for the interface thickness of 100 nm, these equations yield a minimum asphaltenes content of 65% in the "intrinsic" poorly bonded interfacial layer. On the other hand, given that the asphaltenes content cannot be more than 100%, the same equations yield a minimum interfacial thickness of 63 nm.

In conclusion, the "intrinsic" poorly bonded interfacial layer was found to be quite thick and very concentrated in asphaltenes.

FTIR. Figure 4 presents the FTIR transmittance spectrum obtained on a dried sludge emulsion. It shows some similarities with the spectrum obtained on asphaltenes extracted from the supernatant oil (data not presented here, see ref 23). The main features are as follows: (i) large peaks at 2924, 2853, 1461, and 1377 cm^{-1} easily attributed to bending and stretching of aliphatic hydrocarbon groups coming from the entrapped oil, (ii) a small peak at 1700 cm^{-1} characteristic of the stretching of protonated carboxylic acid functions, (iii) a small peak at 1602 cm^{-1} characteristic of aromatic rings stretching, (iv) a small peak at 1032 cm^{-1} sometimes attributed to sulfoxides, and (v) numerous peaks below 1000 cm^{-1} (characteristics of aromatic CH bending).

From these observations, it is concluded that the whole interfacial material mainly contains a mixture of protonated carboxylic acids and asphaltenes.

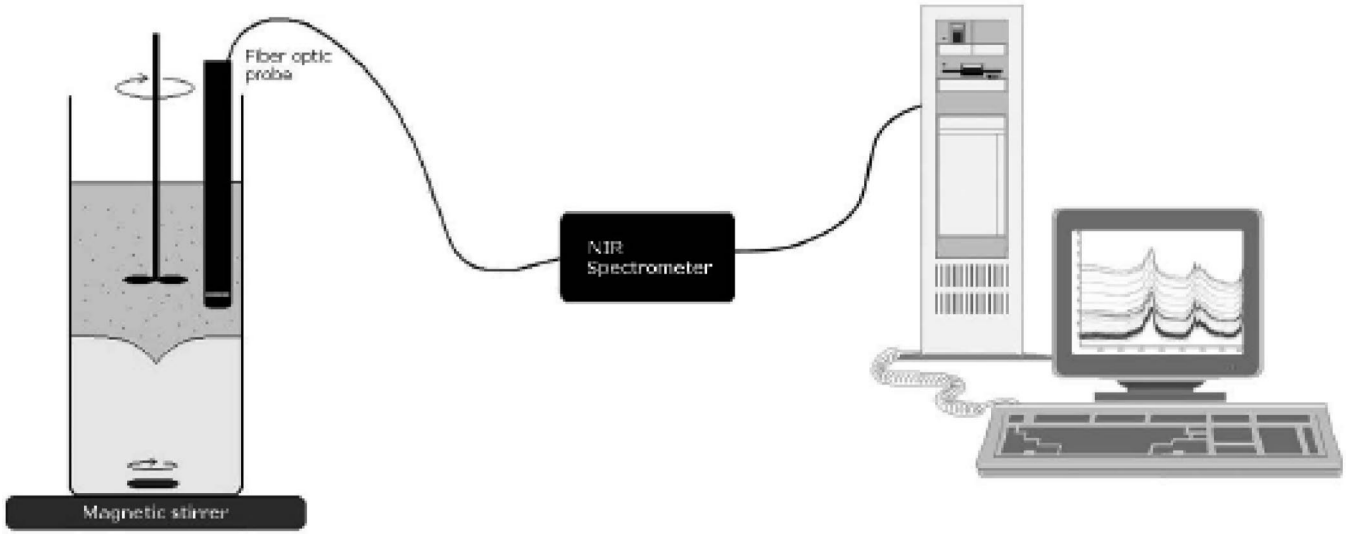

Figure 3. NIR monitoring of particle formation.

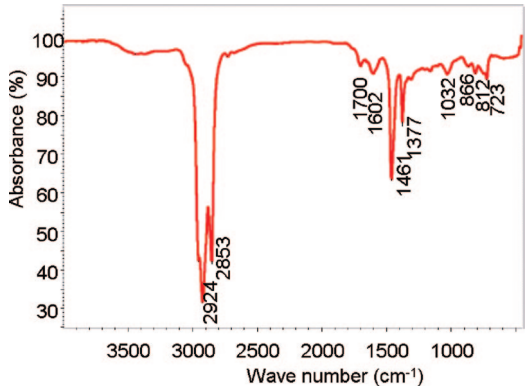

Figure 4. FTIR transmittance spectrum of a dried sludge emulsion.

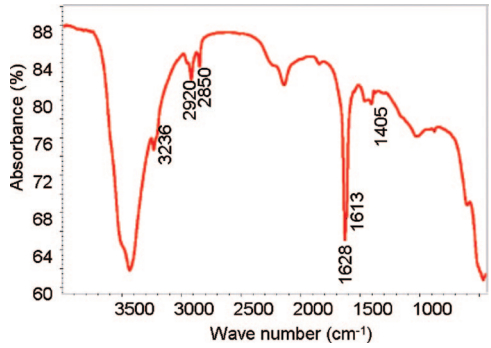

Figure 5. FTIR transmittance spectrum of a dried cleaned sludge emulsion.

Figure 5 presents the FTIR transmittance spectrum obtained on a cleaned emulsion. It is completely different from the previous one and was found to correctly match with a spectrum of tartrate salt from Sigma Aldrich library. The main features are the following: (i) a large band from 2800 to 3600 cm^{-1} in the region of the OH stretch that may correspond to carboxylic acid dimers or residual water, (ii) small peaks at 2920 and 2850 cm^{-1} easily attributed to aliphatic hydrocarbon groups, (iii) a large peak at 1628 cm^{-1} characteristic of the asymmetric stretching of deprotonated carboxylic acid functions with shoulders on both sides that may be due to aromatic rings around 1613 cm^{-1} and to carboxylic acids dimers around 1650 cm^{-1}, (iv) a small peak at 1405 cm^{-1} that, given the presence of the large peak at 1628 cm^{-1}, may be attributed to the symmetric stretching of deprotonated carboxylic acids, and (v) peaks below 700 cm^{-1} that are observed on dicarboxylic acids.

From these observations it is concluded that the "strongly bonded interfacial material" is mainly composed of deprotonated acids, with probably dicarboxylic acids and potentially acid dimers.

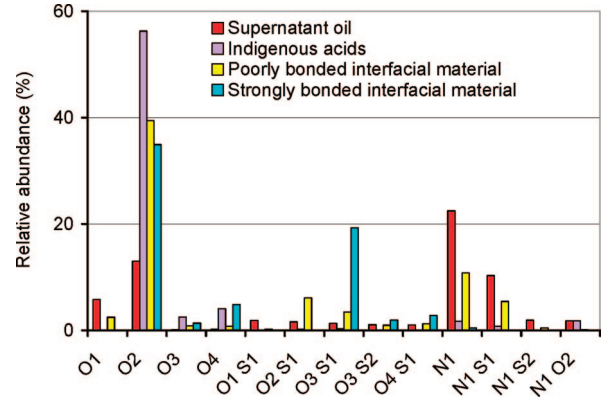

Figure 6. Relative abundance of the main elemental groups in the supernatant oil, the indigenous acids, the poorly bonded interfacial material, and the strongly bonded interfacial material (FT-ICR MS, ESI region).

FT-ICR MS. Figure 6 presents the relative abundance of the different compositional classes identified in the supernatant oil, the indigenous acids, the poorly bonded interfacial material, and the strongly bonded interfacial material. Families are labeled with a reference to the number of heteroatoms ($O_xS_yN_z$).

O_x families are the main constituent of the extracted acids. They are also present in a greater abundance in the interfacial materials than in the crude oil. This reveals a specific adsorption at the water−oil interface. The O_2 family is the most abundant family in both the poorly and strongly bonded interfacial materials, with relative abundances close to the one observed in the extracted acids. It corresponds to monocarboxylic acids. The O_4 family is present in a higher abundance in the strongly bonded interfacial material than in the extracted acids but is present in a lower abundance in the poorly bonded interfacial material. It probably corresponds to the dicarboxylic acids identified in the strongly bonded interfacial material FTIR spectrum. O_xS_y families are almost absent from the extracted acids but are present in a greater abundance in the interfacial materials than in the crude oil. This reveals a specific adsorption

Table 7. Structural Characteristics of the Main Species Identified in the Interfacial Materials (FT-ICR MS, ESI Region)

	O_2	O_4	O_3S_1	O_2S_1
strongly bonded interfacial material	fatty monocarboxylic acids	dicarboxylic acids of all structures (fatty, naphthenic, and aromatic)	non-acidic	0
poorly bonded interfacial material	monocarboxylic acids of all structures (fatty, naphthenic, and aromatic)	0	non-acidic	non-acidic

at the water−oil interface. O_2S_1 species are mostly present in the poorly bonded interfacial material. O_3S_1 species are partitioned between the poorly bonded interfacial material and the strongly bonded interfacial material, with a greater abundance in the latter one. The chemical nature of these compounds is not yet determined. N_z, S_yN_z, and O_xN_z families contain some acids but are present in a lower abundance in the poorly bonded interfacial material than in the crude oil. They are absent in the strongly bonded interfacial material. This reveals a poor adsorption at the water−oil interface. Their detection may even be due to entrapped oil.

These results are very similar to others obtained on water/bitumen interfaces by FT-ICR and showing a specific adsorption of O_x and O_xS_y species in the interfacial material.[16,20]

A more detailed analysis of the mass spectra was conducted as depicted in ref 23. For each chemical class within each sample, the relative abundances of individual signals were plotted versus carbon number and double-bond equivalent (DBE, an indicator of the unsaturation degree of the molecule). Comparing these plots between the different samples provided an indication of the influence of the molecules structure on their specific presence or absence in the interfacial materials. The results are gathered in Table 7. Almost all of the O_2 compounds present in the whole crude are present in the indigenous acids and the poorly bonded interfacial material, without much selectivity on DBE and molecular weight. Contrarily, most of the O_2 compounds present in the strongly bonded interfacial material are fatty acids. O_4 species are almost absent from the poorly bonded interfacial material and are concentrated in the strongly bonded interfacial material without selectivity on DBE and molecular weight. This would be consistent with an increased hydrophilic tendency because of the presence of two carboxylic functions. O_3S_1 species are equally partitioned between the two interfacial layers without a clear influence of their structure. O_2S_1 species are almost absent from the strongly bonded interfacial material and are concentrated in the poorly bonded interfacial material without selectivity on DBE and molecular weight.

Interfacial Activity of Indigenous Acids. Figure 7 presents the dynamic interfacial tension obtained without calcium for various concentrations of indigenous acids and one concentration of the commercial blend from Acros. The indigenous acids promote a significant reduction in interfacial tension between water and toluene: −71% for 1.4 wt %, −52% for 0.1 wt %, and −37% for 0.05 wt %. The magnitude of this reduction is very similar to the one observed on model aromatic monocarboxylic acids and higher than the one observed on a model naphthenic acid.[33] This may indicate that the indigenous acids contain significant amounts of aromatic acids. This analysis is supported by the fact that the commercial blend (mainly composed of fatty and naphthenic acids) has nearly no influence on the interfacial tension.

There is a significant difference, however, between the extracted indigenous acids and the model acids in terms of dynamics: For model acids, the reduction in interfacial tension is almost immediate, but it takes more than 1200 s for the indigenous acids. Such slow dynamics were previously reported for tetra-carboxylic acids.[27]

Figure 8 presents the dynamic interfacial tension measured for a 0.14 wt % solution of indigenous acids when a calcium solution was added to the water bath 500 s after the droplet had been formed. The interfacial tension transiently re-increased from 9 to 16.5 mN/m immediately after the calcium addition but rapidly dropped down back to 11.5 mN/m. This final value indicates that carboxylate salts are stable at the water/toluene interface and have an interfacial activity similar to the one of deprotonated carboxylic acids. The overshoot may indicate that the interfacial layer undergoes a re-organization upon formation of bonds between calcium cations and deprotonated carboxylic acids. Such a perturbation was previously reported for tetra-carboxylic acids.[27]

Another observation, performed at the end of the interfacial tension measurements, supports the parallelism between the indigenous acids and the tetra-carboxylic acids: the presence of a thin cohesive interface upon retraction of the oil droplet into the syringe (Figures 9 and 10). In the case of tetra-carboxylic acids, this cohesive layer is associated with the build up of a 3D cross-linked interfacial layer.

There is a significant difference, however, between tetra-carboxylic acids and indigenous acids regarding the tendency to form particles. While tetra-carboxylic acids rather form a sticky layer at the interface between bulk water and toluene,[27] the indigenous acids form a large amount of particles (Figure

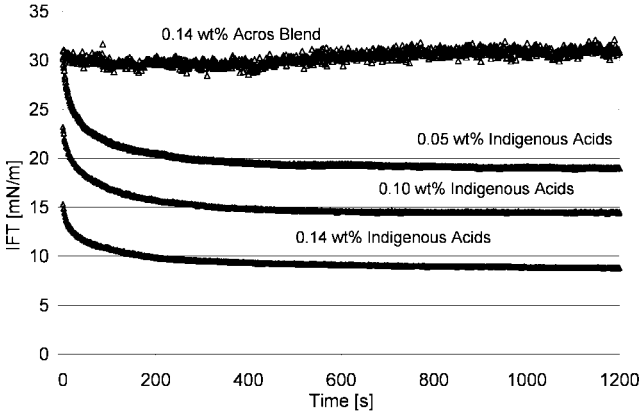

Figure 7. Dynamic interfacial tension between water (pH 9, no calcium) and toluene solutions of acids.

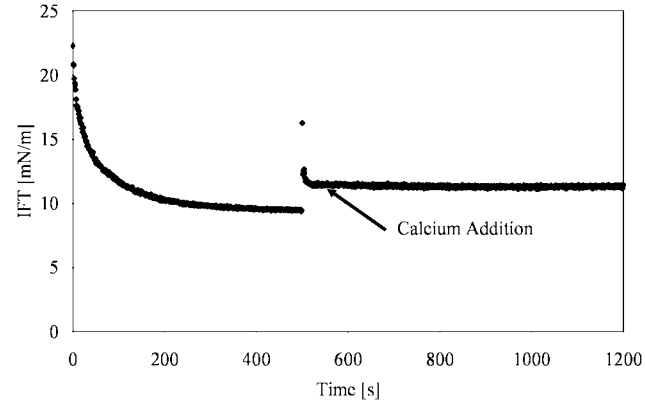

Figure 8. Influence of calcium on interfacial tension for 0.14 wt % indigenous acids in toluene (pH 9, water).

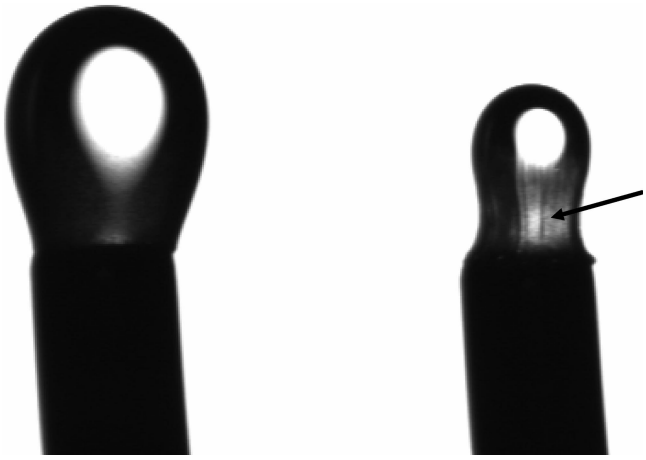

Figure 9. Cohesive interface around a droplet of indigenous acid solution immersed in water (pH 9, calcium) for 20 min. The picture on the left shows the droplet at the size it had during the interfacial tension test. The interface is smooth. The picture on the right shows the same droplet upon suction in the syringe (black cylinder at the bottom). The interface exhibits wrinkles (marked by an arrow), revealing the presence of a layer resisting suction.

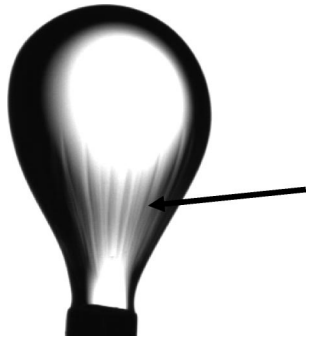

Figure 10. Observation of a cohesive interface around a droplet of tetra-carboxylic acid solution immersed in water (pH 9, calcium) for 20 min [courtesy of Sjöblom from JIP 2 at Norwegian University of Science and Technology (NTNU)]. Upon suction of the droplet in the syringe, the interface exhibits wrinkles (marked by an arrow), revealing the presence of a layer resisting suction.

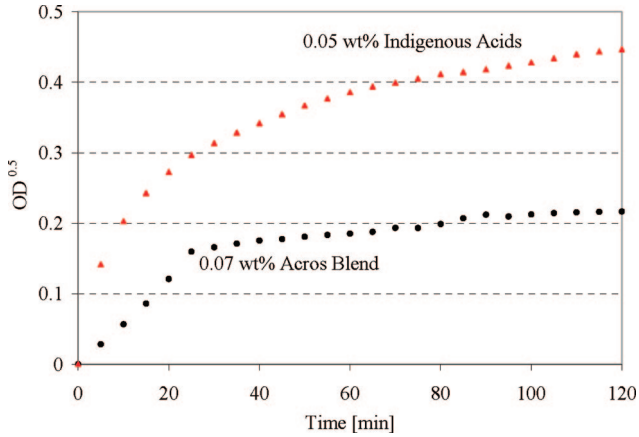

Figure 11. Square root of the optical density versus time for solutions of indigenous and commercial acids.

11). This amount is larger than for the commercial blend from Acros and also for the above-mentioned model acids.[33] This reveals the build up of very strong interactions between carboxylate salts but the inability to form a 3D polymeric network.

Interfacial Rheology. As for the indigenous acids, a cohesive skin was observed around oil droplets immersed in water (for example, Figure 12). This phenomenon was previously reported for asphaltenic systems, with or without identified organic acids.[15] In the present case, the skin was observed in all conditions but was more apparent for high salinity and high pH. In such chemical conditions, when the drop underwent a rapid deflation/inflation cycle with a very large variation of surface, it exhibited very strange shapes (Figure 13), revealing a significant resistance to deformation and probably a high yield strength.

These visual observations were associated to a particular dependency between rheological parameters and frequency. The dilatational modulus was found to be a power law of frequency, and the loss angle was found to be proportional to the corresponding power exponent. This dependency had already

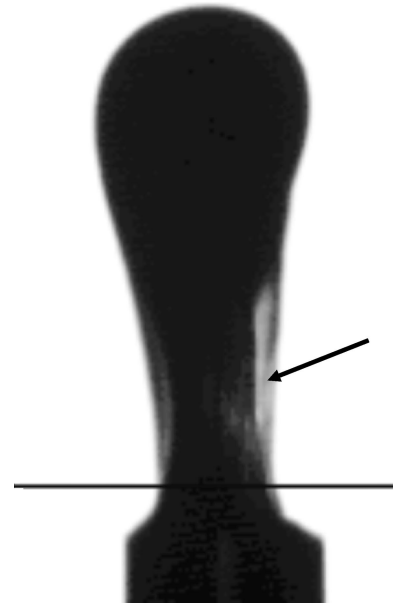

Figure 12. Cohesive interface around an oil droplet immersed in water (after test I). Upon suction of the oil into the syringe, a film appeared (observable by transparency and marked by an arrow) that resisted suction.

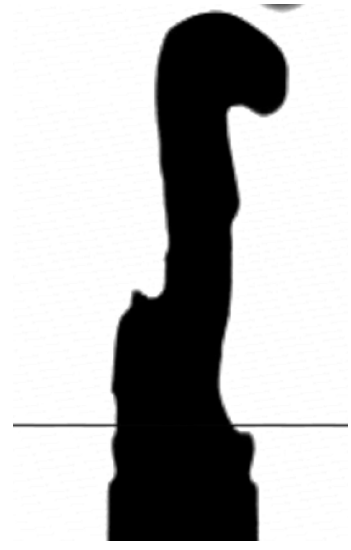

Figure 13. Cohesive interface around an oil droplet immersed in water (after test I). The droplet pictured in Figure 12 was further contracted at a higher rate. The interfacial film exhibited a significant resistance, leading to a strange shape.

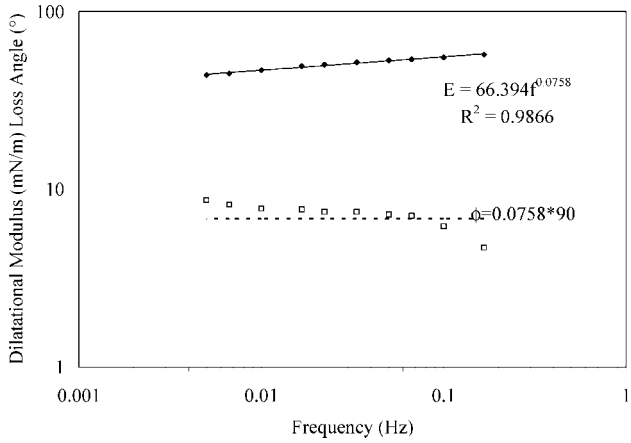

Figure 14. Dependency of rheological parameters with the frequency for a mixed brine (145 g/L $CaCl_2 \cdot 2H_2O$ + 40 g/L NaCl) at pH 8.

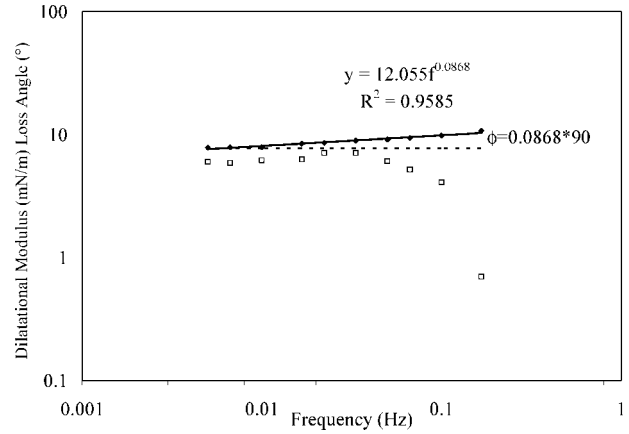

Figure 15. Dependency of rheological parameters with the frequency for deionized water at pH 5.

been observed in the case of asphaltenic oils.[42] It had been attributed to a 2D gel at the interface exhibiting the same rheology as a (3D) polymeric gel at its gelation point

$$E^* = Sf^n e^{in\frac{\pi}{2}} \Leftrightarrow E = Sf^n \text{ and } \varphi = n\frac{\pi}{2} \text{ (rad) or } n\ 90 \text{ (deg)}$$

where f is the oscillation frequency, S is the gel strength, and n is a constant related to the fractal dimension of the gel.[43,44] In the present case, the fit is almost perfect (Figure 14), except in a few cases when the loss angle drops down to very low values (almost 0) at the highest frequencies (Figure 15). This decrease is typical of a frequency-induced glass transition: Above a certain frequency, the time allowed for relaxations to occur is lower than the characteristic time of molecular mobility and the gel behaves like a glassy material.[42] Given the moderate frequencies used during these experiments (maximum of 0.2 Hz), it is likely that the glass transition temperature is not too different from the test temperature (40 °C).

Given the previously reported correlation between the gel strength, glass transition, and emulsion stability,[40] the results are further presented in terms of water chemistry versus four interfacial parameters. The interfacial tension (IFT) related to the packing and the affinity with the interface of the adsorbed species. The gel strength (S) related to the degree of interaction between adsorbed species in the interfacial layer. The loss angle (φ) related to the ratio between elastic and viscous interactions in the interfacial layer. The onset frequency of glass transition (f_T) related to the degree of order in the interfacial layer. Data are summarized in Table 8.

Table 8. Evolution of Rheological Parameters of the Water/Oil Interface with Water Chemistry

test label	IFT (mN/m)	S (mN/m)	φ (deg)	f_T (Hz)
A	27.2	12	7.83	0.05
B	27.5	11	4.113	0.033
C	25.8	8	3.528	0.022
D	27	18	6.057	0.1
E	17	24	11.835	>0.2
F	26	12	7.965	>0.2
G	23.3	11	11.556	>0.2
H	21	23	9	>0.2
I	21	66	68.22	0.2

For nonsalted water (tests A, B, and C), a pH increase from 5 to 8 leads to a decrease in interfacial tension probably associated with a higher dissociation rate of carboxylic acids. The low magnitude of this decrease reveals, however, that the packing at the interface probably decreases because of electrostatic repulsion between ionized molecules. This is confirmed by a decrease in strength, revealing a lower degree of interaction between molecules within the adsorbed layer. The glass transition is meanwhile shifted to lower frequencies, revealing a higher degree of order at the interface, which is expected: All ionized acids show their carboxylic function toward the water phase and align side to side. This evolution is associated with a decrease in loss angle, revealing a relative decrease in viscous interactions compared to elastic interactions, which is coherent with the alignment of acids at the interface.

At pH 7, adding NaCl (tests D and E) decreases the interfacial tension and increases the gel strength, which reveals a better packing at the interface because of a screening of electrostatic repulsion forces by counter-ions. The glass transition meanwhile shifts to higher frequencies, indicating a lower degree of order, and the loss angle increases, indicating a higher relative importance of steric forces. This reveals the adsorption of higher molecular-weight molecules with a lower tendency to form localized interactions. These species are probably asphaltenes.

Contrarily, calcium chloride (test F) does not change the interfacial tension and the gel strength significantly compared to deionized water (test B). This reveals that the increase in packing, because of the electrostatic screening, is hindered. On the other hand, the shift of the glass transition temperature to higher frequencies reveals that the degree of order is low. It probably means that asphaltenes are still present in the interfacial layer. This is confirmed by a higher loss angle compared to deionized water. The packing hindrance may be due to conformational constraints created by the linear linking of acids (particularly dicarboxylic ones) on calcium.

For a mixed brine (tests G, H, and I), an increase in pH from 5 to 8 slightly decreases interfacial tension, strongly increases the gel strength, and slightly decreases the loss angle. The glass transition is shifted to high frequencies. At pH 8 (test I), the formation of a very resistant skin around the oil droplet is associated with a very high value of gel strength. At pH 7 (test H), the mixed brine gives intermediate rheological parameters between the two monotype brines (tests E and F), revealing a combined effect of calcium and sodium rather than a competition. At pH 5, the interfacial tension is lower for the mixed brine (test G) than for the deionized water (test A), revealing a better packing. At pH 5, the gel strength is lower for the mixed brine than for the deionized water but the loss angle is higher. It reveals that, for the mixed brine, the steric interactions

(42) Bouriat, P.; El Kerri, N.; Graciaa, A.; Lachaise, J. *Langmuir* **2004**, *20*, 7459–7464.
(43) Winter, H. H.; Chambon, F. *J. Rheol.* **1986**, *30*, 367–382.
(44) Chambon, F.; Winter, H. H. *J. Rheol.* **1987**, *31*, 683–697.

Table 9. Water Separation Kinetics versus Water Chemistry[a]

time	separated water (%)									
(min)	10.0	20.0	30.0	40.0	50.0	60.0	70.0	80.0	120.0	1440.0
test D	0.0	0.0	0.0	0.0	0.0	0.0	0.1	0.2	0.5	1.7
test E	0.0	0.0	0.0	0.3	0.3	0.3	0.9	1.4	3.0	5.9
test F	0.0	0.4	0.7	0.9	1.2	1.5	1.9	2.1	2.8	39.3
test G	0.0	3.8	5.6	6.9	21.8	26.0	30.4	30.6	30.6	63.9
test H	0.0	0.0	0.0	0.0	0.0	0.4	1.3	2.4	4.2	44.8
test I	1.2	1.8	3.2	3.6	3.6	3.6	3.6	3.6	3.6	24.8

[a] See correspondence with test labels in Table 4.

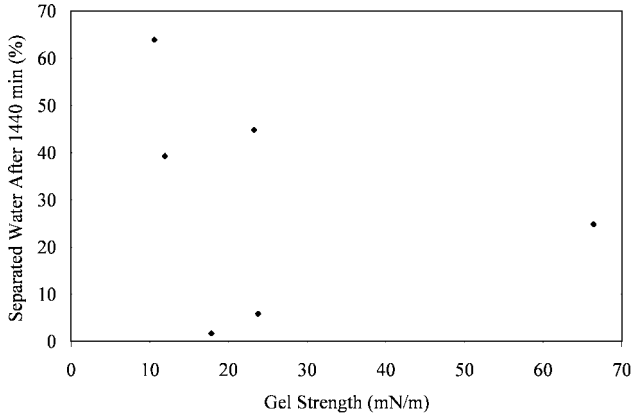

Figure 16. Final water separation versus gel strength.

dominate the localized interactions. It may be due to the fact that the competition between acids and asphaltenes is not favorable to acids when they are poorly deprotonated.

Emulsion Stability. Table 9 presents the water separation data obtained for the various brines. For a mixed brine, an increase in pH from 5 to 8 (tests G, H, and I) greatly reduces the water separation, which follows the corresponding increase in gel strength. Contrarily, at pH 7, the water separation is very small for the NaCl monotype brines (tests D and E) and far higher for the $CaCl_2$-containing brines (both monotype and mixed; tests F and H), which does not follow the evolution of the gel strength. Experiments were repeated but gave similar results.

A correlation between the water separation after 12 h and the different rheological parameters was investigated (Figure 16) but was not found. The reason for this absence may be due to the complexity of the mechanisms involved at the interface. The rheological parameters were measured after a very long time, allowing for a full effect of all of the mechanisms. Contrarily, the emulsion tests were performed after shaking for a few minutes, only allowing for the fastest mechanisms to produce their effects. The fastest mechanisms are most likely the dissociation of acids because of pH and, to a less extent, the packing of asphaltenes because of salinity. Contrarily, the reaction of calcium on acids was found to transiently disorganize the interfacial layer (Figure 8). Consequently, the packing hindrance effect observed with calcium chloride may be more intense for a fresh emulsion than for an aged brine.

Discussion

The comparison between the FTIR spectra and the results on TAN/asphaltenes tends to indicate that the whole interfacial material is mainly composed of a thick poorly bonded interfacial material dominated by asphaltenes. Quantitatively, organic acids are mainly present in the poorly bonded interfacial material under the protonated form but in relatively low concentration. Qualitatively, organic acids (and among them dicarboxylic acids) are probably of great importance for the interface stability, because, under the deprotonated form, they constitute almost exclusively the "strongly bonded interface". The quantitative predominance of protonated acids over deprotonated ones in the poorly bonded interfacial material may indicate a particular adsorption mechanism. Given that the pH of the water phase is 1.5 over the pK_a of naphthenic acids, almost all of the acids coming in the vicinity of the interface should be deprotonated, whatever their later behavior (in solution in water, in solution in oil, or stable at the interface). This may mean that the acids present in the poorly bonded interfacial material never directly contacted the water phase and are not concentrated at the interface because of their own hydrophilic behavior. Alternatively, it was found that the asphaltenes extracted from the supernatant oil contained notable amounts of acids (data not presented here, see ref 23), which suggests that acids and asphaltenes co-precipitate and further co-adsorb at the interface. Similar conclusions can be found in refs 20 and 22. The influence of these co-precipitated acids on the emulsion-stabilizing behavior of asphaltenes is unknown. They may influence the polarity and size of asphaltenes flocculates.

The FT-ICR MS spectra confirm the presence of carboxylic acids (O_x species) at the interface together with sulfur-containing non-acidic species (O_xS_y) of an unknown nature. Using the same techniques, similar findings were also reported elsewhere.[15,16,20] Carboxylic acids are partitioned between the two interfacial materials depending upon their structure. Fatty monocarboxylic acids are found in both interfacial materials, with a preference for the strongly bonded interfacial material, which is in agreement with the previous descriptions of the interface in soap emulsions.[12,13] Unsaturated monocarboxylic acids are found exclusively in the poorly bonded interfacial material, which is coherent with the co-precipitation phenomenon described above: These acids are the most chemically compatible with asphaltenes, which are generally assumed to be polyaromatic compounds. Dicarboxylic acids of all structures are found exclusively in the strongly bonded interfacial material, because of their higher hydrophilic tendency. As a result, they create a strongly bonded interface, with a high degree of unsaturation, which is favorable for the further adsorption of asphaltenes at the water/oil interface.

The indigenous acids appear to have a far higher interfacial activity than a commercial blend, mainly composed of fatty acids. Their activity is intermediate between model unsaturated acids and tetra-carboxylic acids. This tends to indicate that the fatty acids found in the strongly bonded interfacial material do not play an important role. Alternatively, the presence of traces of tetra-carboxylic acids was specifically investigated by FT-ICR MS and high-performance liquid chromatography (HPLC) and was discarded. It is suspected that the interfacial behavior of indigenous acids is strongly influenced by dicarboxylic acids that can undergo a linear linking on calcium cations and, therefore, create a cohesive interface.

Such a cohesive interface was also observed with both a toluene solution of indigenous acids and the whole crude oil. The corresponding interfacial rheology was found to be the one of a 2D gel close to its gelation point. The variation of the rheological parameters with pH, salinity, and type of cations revealed complex interactions between asphaltenes and acids, as reported in ref 21. The kinetic differences between the involved mechanisms does not allow for a direct correlation between the rheological parameters and the emulsion stability measured after different aging times.

Some organization phenomena reported by others[17,19] were

investigated but could not be observed (absence of birefringence in the samples).

Conclusion

A comprehensive study of the influence of organic acids on the emulsion stability of a low-TAN/high-asphaltenes crude oil led to the conclusion of a strong interaction between asphaltenes and acids. A 2-fold scenario is proposed but needs further investigation. On one hand, unsaturated monocarboxylic acids precipitate with asphaltenes and co-adsorb at the water/oil interface. Alternatively, dicarboxylic acids specifically adsorb at the interface and form naphthenate salts, thereby creating a first layer favoring the further adsorption of asphaltenes. These mechanisms lead to the formation of a very cohesive interfacial layer with a 2D gel rheology. This gel is suspected of exhibiting a glass transition and a yield strength severely hindering droplets coalescence and water separation.

These observations allow for the proposal of a supplement to the previously mentioned description of the influence of organic acids on emulsions:[8] (i) By themselves, unsaturated monoacids do not contribute significantly to the interface because of their high chemical affinity with bulk oil (predominantly of naphthenic and aromatic nature). They can co-precipitate with asphaltenes. In such a case, they may increase the affinity of asphaltenes flocculates with the water surface and favor stable emulsions. (ii) Fatty acids specifically adsorb at the interface because of their low chemical affinity with bulk oil. If the oil contains enough fatty acids or a combination of fatty acids and paraffin, this leads to the formation of a strong interface and to soap emulsions at near neutral pH values. Contrarily, if the oil contains significant amounts of asphaltenes, there will be a competition between asphaltenes and fatty acids at the interface. Asphaltenes will stabilize the interface at acidic pH, and fatty acids will remove asphaltenes from the interface at neutral pH. This leads to a minimum in emulsion stability at near neutral pH values. (iii) Di-acids specifically adsorb at the interface regardless of their saturation degree and favor the adsorption of asphaltenes, leading to very tight emulsions at near neutral pH values.

Acknowledgment. The authors acknowledge Saudi Aramco for the permission to publish these results as well as Ann Mari Hanneset (NTNU) and NagoorPitchal MeeranPillai (Saudi Aramco) for undertaking certain laboratory experiments. Dr. Sebastien Duval (Saudi Aramco) is also acknowledged for his constant support and scientific advice.

EF800615E